

Stacked Electromagnetic Band Gap Ground Optimization for Low profile Patch Antenna Design

P. Saleem Akram, T.V. Ramana

Abstract: Current paper concentrates on the design and analysis of novel stacked Electromagnetic Band Gap structures. The surface properties of both the novel designs, for instance, High surface impedance (HSI), Artificial Magnetic Conductor (AMC) and Forbidden band gap (FBG) are overseen by utilizing Finite element method (FEM) based 3D electromagnetic (EM) simulator. The acquired outcomes are contrasted with the outcomes of classical mushroom EBG structure. Proposed novel structures are named here as Progressive Stacked Electromagnetic Band Gap (PSEBG) and Stacked Electromagnetic Band Gap (SEBG). The unit cell of SEBG and PSEBG are analogue to MEBG structure, incorporates two layers over the principle plane. Top layer is a planar MEBG, middle layer contains cluster of small square MEBGs. Both proposed and reference structures are applied as ground plane to microstrip patch antenna (MPA). Radiation characteristics return loss, Front to back radiation, compact and low profile properties are studied and presented to optimize the best EBG.

Key words: Electromagnetic (EM), Mushroom Electromagnetic Band Gap (MEBG), Artificial Magnetic Conductor (AMC), forbidden band gap (FBG).

I. INTRODUCTION

The colossal progression in antenna engineering empowers the design of diminished antenna [1, 2] structures with enhanced performance characteristics. Distinctive techniques [3-9] have been proposed for scaling down of antennas, for instance, utilization of higher permittivity dielectric substrates or meandering paths or fractal shape antennas. Regardless, these were enduring with limited antenna band-width and ohmic losses (fractal shapes antennas). The novel properties of EBGs, demonstrating solution to the issues, thusly antennas are embedded by EBG surfaces [9-13]. EBGs are the periodic array of EM structures engraved on metal backed dielectric substrate. The periodicity of an array is electrically small, and additionally the dimensions of the individual particles in the unit cell (UC). Architecture and individual dimensions of elements expect key occupation in designing of any EBG and blend of its frequency response. Usually patch shapes appear in squared [14], hexagonal [15] and rectangular [16] shapes. EBG exhibits two enrapturing behaviors: one is AMC, in which reflection phase is close or equivalent zero. Another is FBG, in which proliferation of surface wave long the surface is nullified.

Manuscript published on 28 February 2019.

* Correspondence Author (s)

Dr. T. V. Ramana*, Associate Professor, ECE Dept. at GITAM University, Visakhapatnam (A.P), India.

P. Saleem Akram, Asst. Prof., Department of ECE, KLEF, Vaddeswaram, Guntur, GITAM University, Visakhapatnam (A.P), India.

© The Authors. Published by Blue Eyes Intelligence Engineering and Sciences Publication (BEIESP). This is an open access article under the CC-BY-NC-ND license <http://creativecommons.org/licenses/by-nc-nd/4.0/>

The AMC behavior occurs by prudence of very HSI in a particular range of frequency, amidst which the tangential electric field components are diminutive; prompting a few fascinating applications in the antenna field [14-19]. In addition, contingent upon the geometry of the UC, both behaviors may show up in a similar frequency extend [20, 21]. The AMC property helps in delineating of compact antennas, as the image currents appear in zero degree phases, thus, antennas can be set parallel and near the EBG ground [22]. The FBG property of EBG improves the antenna radiation patterns [14, 15]. So as to minimize the aperture of antenna and enhance its performance regarding of gain and efficiency, it is feasible to use the concept of EBG [14]. Various experimental methods for describing the EM properties of EBGs were thought about [23, 24]. The goal is to propose two novel stacked EBG structures and depict its properties. To confine ground plane size as well as profile of radiating antenna without extending back radiation. Finally, the performance of low profile MPA over the proposed SEBG and PSEBG ground surfaces are studied and presented. The idea of stacked EBG surface has been presented in [14], where the author utilized three layer structures for size reduction of unit cell. Concealment of noise in parallel plate waveguide was done by utilizing stacked EBG structures in [25]. The examination of band gap properties in double layered dipole and triple arrays is presented in [26]. The fundamental EBG structure comprises of periodic array of dielectric or metallic patches in one, two or three dimensions, engraved on one side of dielectric where opposite side contains metallic ground. This controls the spread of EM waves at specific angles of incidence at few frequencies hence called partial band gap, if the propagation of EM waves isn't permitted in every direction then they are called universal band gap [27, 28]. In this paper, MEBG is picked as a base for designing of novel SEBG and PSEBGs, since it has been considered broadly in literature. The proposed models are created by placing a planar MEBG structure over an assortment of compact MEBGs. The FBG and AMC properties of proposed models rely upon its UC parameters. The FBG is impacted with the parameters of both the middle and top MEBGs, where as the in-phase reflection character depends essentially on the measurements of the top MEBG, particularly the architecture of the patch [29].

II. DESIGN OF MEBG, SEBG & PSEBG UC'S

The UCs of MEBG, SEBG and PSEBG are depicted from Figure 1 to 3, where the MEBG is taken as reference, because it was studied extensively in literature.

Both proposed and reference EBG UC architectures are composed on FR4 substrate having 4.4 relative permittivity and a thickness of 124mil (3.2mm). The cross section in Figure 1

comprises a patch of 17.5X17.5 mm² imprinted on FR4 substrate's top layer, while opposite face contains metallic ground. A metallic via with 0.475mm radius shorts the patches lying in top and middle layers with bottom ground. The stub is located at the center to each patch. Figure 2 is depicting SEBG UC. It comprises of square shaped patches orchestrated in stacked, where middle layer having a height of 1.6mm contains cluster of four compact square patches each of 3.4X3.4mm², arranged at its all corners, above to them at a tallness of 3.2mm patch of measurement 17.5X17.5 mm² is placed. Every one of these protrusions is associated with ground lying on the opposite face of FR4 by a metallic via of 0.475mm radius. The cross section in figure 3 comprises of patches stacked vertically, where middle layer comprises array of compacted progressive protrusions, the assortment of protrusions lying at all corners of a UC whose measurement is 3.4X3.4mm². Latter, assortment of protrusions set corner to corner with a measurement of 3.075X3.075mm². Each one of these patches is kept at a stature of 62mil (1.6mm) above the ground. As explained above here also via with 0.475mm radius is used to short patches lying in both middle and top layers to bottom ground. Top layer resembles what is cleared up in figure 2. In this examination, to restrict the EBG UC measure, the author picked FR4 substrate of 3.2mm stature. Otherwise, the AMC metallization also energized as like an antenna by the feed line, if the extent of EBG UC is identical or more noteworthy than the radiating patches. The measurements of all the three structures are summarized in table I.

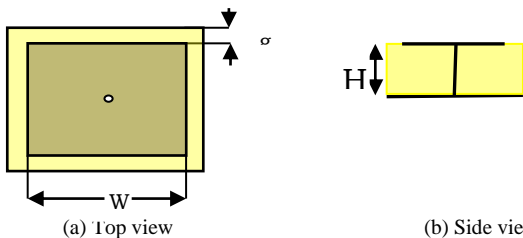


Fig. 1. Model of MEBG unit cell. Include a square protrusion on top face of FR4 substrate backed by a ground. Via shorts patch with ground.

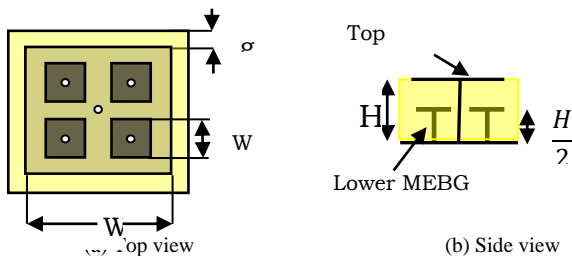


Fig. 2. Model of SEBG UC, contains square patches arranged in stacked and imprinted on FR4 substrate. Via shorts all patches with ground.

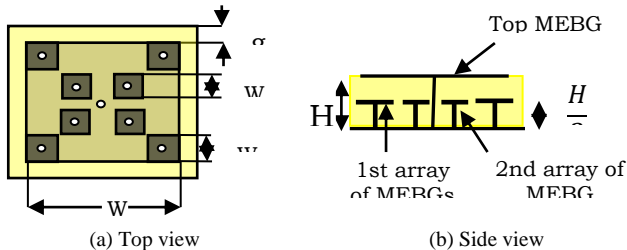


Fig. 3. Model of PSEBG UC.

TABLE I DIMENSIONS OF MEBG, SEBG & PSEBG UCs.

Name of Parameter	Symbol	MEBG	SEBG	PSEBG
Square patches	W X W	17.5X17.5 mm ²	17.5X17.5 mm ²	17.5X17.5 mm ²
	W1 X W1		3.4X3.4 mm ²	3.4X3.4 mm ²
	W2 X W2			3.075X3.075 mm ²
Gap	G	1mm	1mm	1mm
Stub radius	R	0.475mm	0.475mm	0.475mm
Dielectric substrate height	H	3.2mm	3.2mm	3.3mm

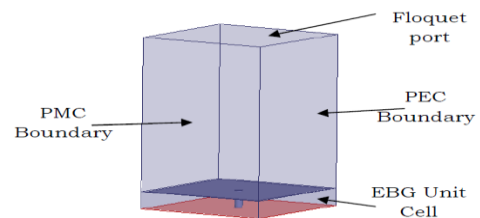
For better comparison of simulated outcome of MEBG, SEBG and PSEBG UC, its key parameters like substrate thickness, measurement of patch, gap and substrate material are viewed as indistinguishable, with the goal that their frequency of resonance will stay consistent and meet. So further vital characteristics, for example, AMC and FBG can be effectively looked at.

III. ANALYSIS OF MEBG, SEBG & PSEBG STRUCTURES

Various techniques were accessible in literature to investigate the characteristics of any EBG UC. They were comprehensively grouped into four classifications [30]: 1) Lumped element circuit model [14], 2) Transmission line model [31], 3) Computational EM modeling using of full wave solvers. On account of many-sided quality of EBG structures, it is generally hard to portray them with first two techniques. 3D-EM simulators using advanced numerical techniques, prevalently utilized in examination of EBG structures. During the study, AMC, HSI and dispersion features of reference model and proposed novel models (i.e. SEBG and PSEBG) are analyzed and determined in this paper using HFSS.

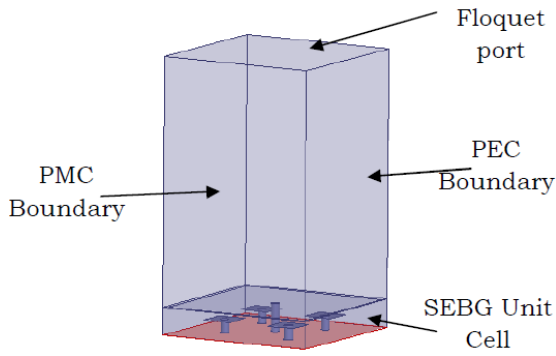
A. Determination of AMC behavior

EBG structure exhibiting an unordinary however vital property which is named as AMC. To decide the coefficient of reflection phase property of above discussed three EBG models, respective UCs ought to be applied with perfect electric conductor (PEC) and perfect magnetic conductor (PMC) boundaries alternately on its four faces. To exhibit the impact of intermittent imitation in an unbounded cluster configuration, wave port is de-inserted on UC's top face. The entire reenactment arrangement is appeared in Figure 4.

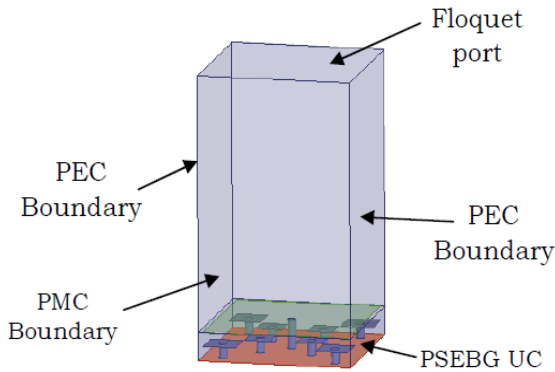


(a) Simulation setup for MEBG unit cell.





(b) Simulation setup for SEBG unit cell



(c) Simulation setup to determine AMC behaviour of PSEBG UC.
Fig. 4. AMC and High impedance properties measurement setup.

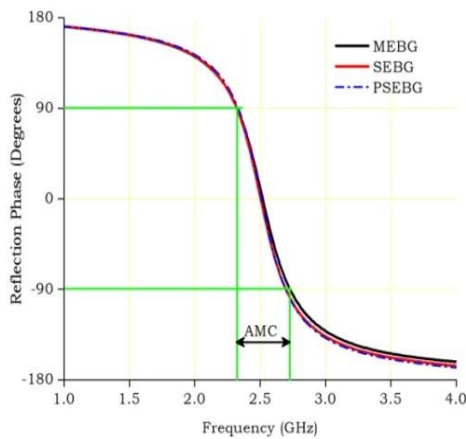


Fig. 5. Coefficient of Reflection phase diagram for MEBG, SEBG & PSEBG UCs.

Figure 5 exhibits the reflection phase coefficient for MEBG, SEBG and PSEBG UCs, under normal incident plane waves. It goes relentlessly from $+180^\circ$ to -180° with respect to the frequency. The frequency at which the phase of reflection is nil is considered as the center frequency of that UC. At and near the center frequency, in a particular range, the impedance of corresponding UC is greater than or equivalent to free space impedance, then coefficient of reflection is +1. Reflected waves meddle with the episode wave's in-phase during the state of $+90^\circ$ to -90° hence named as AMC region. Outside the AMC region EBG exhibits comparable reflection phase attributes [41 – 43] as

those of a regular PEC. Subsequently, any antenna working inside the AMC region can be placed directly over the proposed EBG ground without getting shorted. This integrated architecture upgrades the radiation attributes of the mounted antenna. The resonance frequency, AMC band width of MEBG, SEBG and PSEBG are determined its reflection phase diagram appeared in figure 5, and are portrayed in Table II.

TABLE II AMC BAND GAP COMPARISON OF MEBG, SEBG & PSEBG UCs.

Parameter Name	MEBG	SEBG	PSEBG
Resonant frequency	2.5GHz	2.5GHz	2.5GHz
AMC band gap	404.2MHz	373.8MHz	364.4MHz
Fractional band gap	16.17%	14.95%	14.58%

B. High impedance region

At and around the operating frequency, the EBGs are exhibiting low loss reactive surface, where its impedance is abnormal unlike conventional metal grounds. The high impedance reactive region of MEBG, SEBG and PSEBG structures is shown in figure 4. Low volume antennas can be developed using high impedance property of EBG.

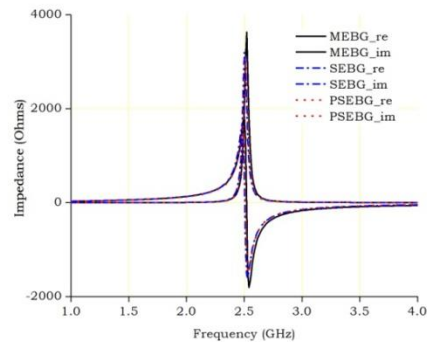


Fig. 6. HSI characterization of three UCs.

C. Analysis of FBG

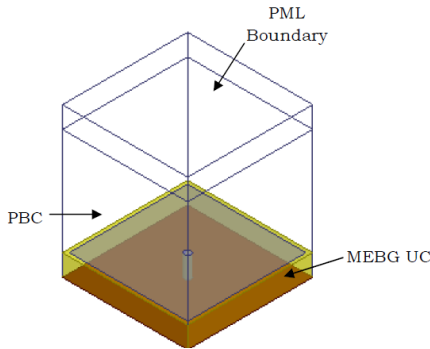
The EBG can't be differentiated completely by its surface properties, when EM waves are incident normal to EBG surface. So, to determine surface wave band region, as well as pass band and stop band ranges of any EBG, its FBG property is utilized. Usually, FBG range [40] is determined with the help of dispersion diagram derived from the respective EBG UC [44 – 47].

The simulation methodology comprises of a perfect matched layer (PML) boundary which is characterized on the top face of the UC to imply free space over the UC.

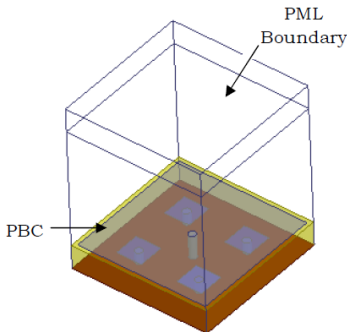
Whereas, four side walls are applied intermittently by PMC and PEC boundaries [48, 49].

The entire estimation process of three UC models demonstrated in figure 7. Γ -X direction of proliferation [32] of EM wave is considered for explanation. The dispersion diagram contains first scattering mode (This is named as TM mode, its outrageous value demonstrates the lower frequency limit of band gap) and second scattering mode (named as TE mode).

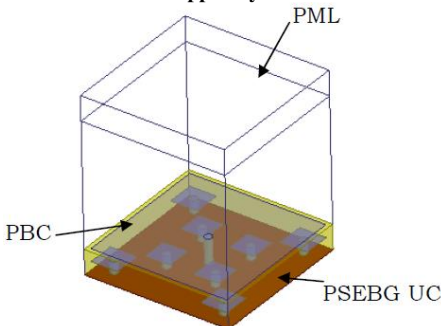
The intersection of TE mode with the light line indicates the maximum furthest frequency band gap. By inspecting the territory between the lower and maximum furthest frequency points determines the band gap. During this band gap neither TE not TM surface wave's proliferation is hindered.



(a) UC of MEBG applied intermittently by PMC and PEC boundaries and topped by PML.

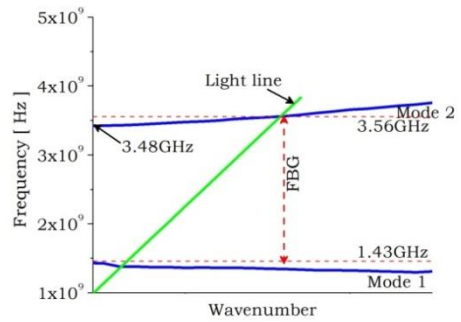


(b) UC of SEBG applied intermittently by PMC and PEC boundaries and topped by PML.

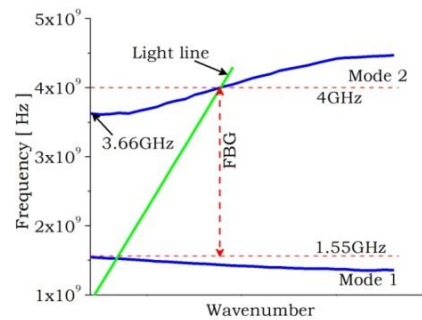


(c) UC of PSEBG applied intermittently by PMC and PEC boundaries and topped by PML.

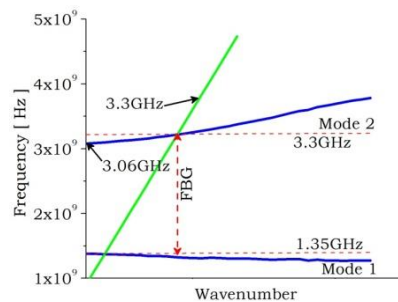
Fig. 7. Simulation setup to measure FBG property of three EBG models.



(a) Dispersion diagram of MEBG



(b) Dispersion diagram of SEBG.



(c) Dispersion diagram of PSEBG.

Fig. 8. Dispersion diagram for three EBG models.

Figure 8 shows the dispersion diagrams of all three EBG models, which determines the FBG of respective UC. Following perceptions produced using dispersion diagram; that is, beneath the center frequency, the EBG structures bolsters TM waves, at high frequencies, it bolsters TE surface waves.

The EBG is exhibiting high surface impedance at the resonance frequency hence respective EBG's group velocity is low for both TE and TM waves. The range between TM and TE bands is characterized FBG. The TE waves, that are lying above and left to the light line, in a short range of frequency, viewed as radiative, leaky modes, these transmit beneficially into free space exactly when their phase matches with the phase of the plane wave along the interface. Figures 6(a) to 6(c) are demonstrating the FBG of

MEBG, SEBG and PSEBG models. Table III delineates the measured results, where fractional estimation of FBG is lessening from MEBG to PSEBG.

TABLE III COMPARISON OF FBG BAND GAP OF MEBG, SEBG AND PSEBG UNIT CELLS.

Parameter Name	MEBG	SEBG	PSEBG
Mode 1	1.55GHz	1.43GHz	1.35GHz
Mode 2	4GHz	3.56GHz	3.3GHz
FBG	2.45GHz	2.13GHz	1.95GHz
Fractional FBG	98%	85.2%	78%

From obtained results it can be conclude that anyEBG structure never permits neither TE nor TM surface waves. This helps to avoid the interference between radiated waves of antenna and surface waves. So, distortion can be eliminated.

IV. LOW PROFILE ANTENNA DESIGN

EBG structures are utilized broadly as ground plane to enhance antenna performance [33-39]. Contrasted with a flat metal ground plane, an EBG ground plane forestalls proliferation of surface waves, prompts less in reverse radiation of an antenna. In this manner wastage of power in unintended direction is decreased. In literature different techniques have proposed for low profile applications. In this paper, analyst meant to choose best EBG ground so low profile antenna with improved radiation attributes can create with least back radiation. In literature, there exist so many EBG ground architectures. For our study author considered two most popular architectures which were produced better results when compared to all other models. The results obtained in proposed EBG ground model are compared with the results of two popular architectures.

For better comparison of results both the popular models are redesigned at center frequency of 2.5GHz. At first each of the three models are designed and studied utilizing MEBG unit cells. After optimization of the best MEBG ground, it is supplanted by, firstly SEBG and later PSEBG UCs ground to study its impact on the patch performance. The MEBG, SEBG and PSEBG UC and patch antenna are focused at 2.5GHz. First of all, the rectangular patch antenna is collinearly surrounded by array of MEBG UCs from its three sides, second, a 3X3 array of MEBG UCs lying underneath and covering the total footprint of patch aperture and third, an array of MEBG UCs lying under the patch yet set closer to its radiating edges (proposed model) are considered. All these arrangements are designed and simulated in Ansoft HFSS to comprehend the effect of MEBG ground structures on radiation characteristics of an antenna. A customary linear polarized rectangular patch antenna has a footprint of 33.3X27.6 mm² with edge feeding, is imprinted on top face of FR4 substrate of thickness 1.6mm, while back face contains regular conducting ground of 116X59 mm².

From simulated results the resonating bandwidth of 63MHz (fractional band width of 2.52%) at 2.5GHz and gain of 2.93dB can be observed. These outcomes are utilized as a source of perspective for comparison of MEBG grounded results in ensuing section.

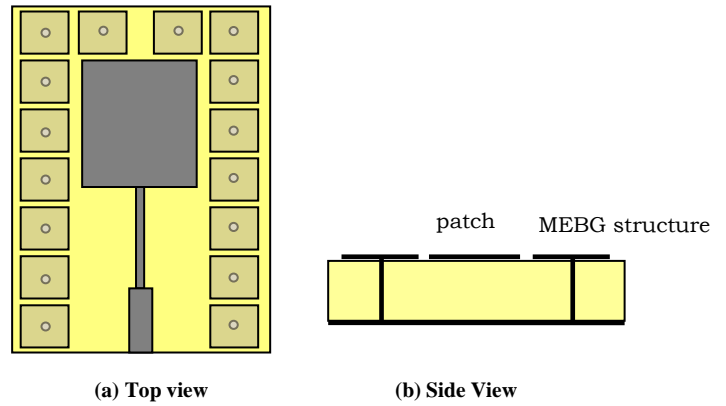


Fig. 9. Rectangular patch antenna surrounded by MEBG unit cells.

The radiating patch is surrounded by a layer of MEBG UCs [36], as shown in figure 9. The FBG [40] and AMC band gaps of MEBG covers the entire frequency band gap (S11>-10dB) of patch. Hence the surface waves excited by this patch antenna are controlled from propagation and also its image currents will be in-phase with radiating currents. The new antenna has dimensions of 32.4X27.2mm², lies co-linear with MEBG ground of 94.3X73 mm² and achieved good matching of 50ohm at 2.5GHz with 97.7MHz (fractional band width of 3.9%) bandwidth and gain of 5.37dB. The complete structure has a thickness of 3.2mm. This design enhances the gain by 2.8dB and fractional bandwidth by 1.38% when compared with conventional design. In this method, the aperture of antenna is scaled down along its length by 2.7%, along its width by 1.44% and ground is scaled down by 18.7% along its length and along its width, the size of ground is increased by 23%. The increase in overall size of antenna ground makes the antenna bulky. Table IV presents the similar kind of works available in literature and its results for better evaluation of designed model.

TABLE IV Comparison of designed model results with literature results contains microstrip patch antenna surrounded by EBG unit cells.

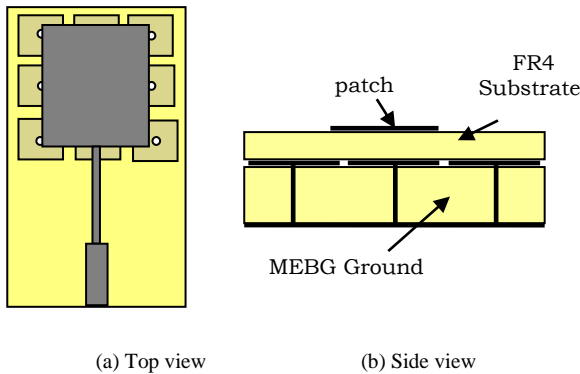
Reference No.	[41]	[42]	[43]	Designed Model
EBG size	1054X1054 μm ²	2.04X2.04 mm ²	Special Model	MEBG
Thickness	510μm	1.575mm	1.575mm	3.2mm
FBG (GHz)	31.3-59.8	Not given	2.45- 2.55	1.55-2.45
AMC	2.85GHz	Not given	~120MHz	404.25MHz
Gain	5dB	5.4dB	7dB	5.4dB
Back radiation	Not given	Not given	Not given	-13dB
Operating band width	15%	~8%	3.05%	3.9%

Next, the 3X3 array of MEBG UCs kept underneath (behind) the antenna to cover the whole footprint of patch as appeared in figure 10. The new antenna contains three layers (top layer contains patch, center layer contains substrate, base layer contains MEBG ground) and total height of 4.8mm (186mil).



Stacked Electromagnetic Band Gap ground Optimization for low profile patch antenna design

The patch antenna lying above and in parallel with resonating MEBG structures, the pooled geometry resonate at a much lower frequency. To bring resonance frequency back to unique (2.5GHz) the antenna footprint over the 3X3 array MEBG ground is downsized along its length by 17%, along its width by 18.4%. The ground is downsized by 19.6% along its length and along its width by 6%. The final antenna has footprint of 27.7X22.5mm², over the 3X3 MEBG ground of 93.3X55.5 mm² and showing 102.3MHz (fractional band width of 4.08%) bandwidth at 2.5GHz and gain of 5.63dB. This design improves the bandwidth by 1.56% and gain by 2.7dB contrasted with conventional method. Table V recorded the comparative kind (backed EBG) of works accessible in literature for better examination of designed model.



(a) Top view (b) Side view
Fig. 10. 3X3 array of MEBG UCs as a ground placed underneath the rectangular patch antenna.

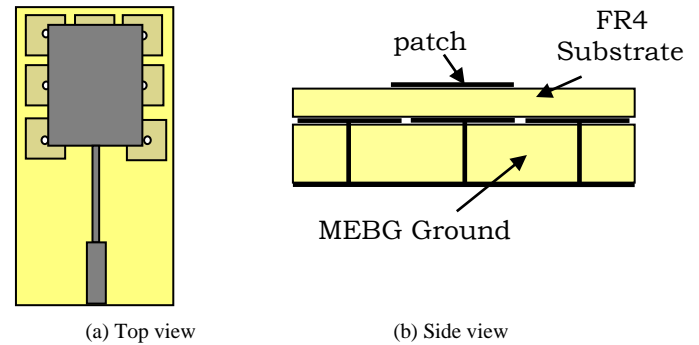
TABLE V

COMPARISON OF DESIGNED MODEL RESULTS WITH LITERATURE RESULTS CONTAINS MICROSTRIP PATCH ANTENNA BACKED BY 7X7 EBG UNIT CELLS [37], DIPOLE ANTENNA BACKED BY EBG ARRAY [38], AND FRACTAL ANTENNA BACKED BY EBG ARRAY [39].

Reference No.	[37]	[38]	[39]	Designed Model
EBG size	4.5X4.5 mm ²	7.3X7.3 mm ²	14.6X14.6 mm ²	17.5X17.5 mm ²
Gap	2.5mm	1.3mm	0.5mm	1mm
Thickness	1.5748 mm	Not given	2mm	3.2mm
Radius of Via	0.2mm	0.4mm	0.25mm	0.475mm
FBG (GHz)	4.41- 6.1	4.6-6.4	Not Given	1.55-2.45
AMC (GHz)	Not given	4.6-6.4	24.4-24.53	404.25 MHz
Gain	3.75dBi	4.8dBi	6.12 dBi	5.63dB
Back radiation	-15dBi	Not given	Not given	-12dB
Operating band width	Not given	50MHz	120MHz	102.3MHz

Next, the proposed MEBG ground model, which is the altered variant of 3X3 array MEBG ground, where MEBG UCs are set behind and closer to the edges of radiating patch as opposed to covering the entire footprint of patch. The total arrangement appeared in figure 11. This arrangement also confines the surface wave proliferation and image currents will be in-phase. Now antenna has a footprint of 27.3X22.1mm², over the proposed MEBG ground of 92.3X55.5mm², displaying 130.9MHz (fractional band width of 5.22%) bandwidth at 2.5GHz and a gain of 6.08dB. In this strategy the size of radiating patch is downsized by 18% along its length and 19.9% along its width. The ground is downsized by 20.43% along its length

and along its width by 6%. In this strategy band width of 2.7% and gain of 3.15dB improved contrasted with traditional design.



(a) Top view (b) Side view
Fig. 11. MEBG UCs placed nearer to radiating edges and underneath the patch antenna.

TABLE VI
 SUMMARY OF PROPOSED DESIGNED RESULTS.

Parameter	Proposed Model results
EBG size	17.5X17.5 mm ²
Gap	1mm
Thickness	3.2mm
Radius of Via	0.475mm
FBG (GHz)	1.55-2.45
AMC (GHz)	404.25 MHz
Gain	6.08dB
Back radiation	-11.5dB
Operating band width (Fractional)	5.22%

From above results it can be concluded that the model proposed in figure 11 is best choice for design of low profile patch antennas. The summary of simulated results starting from rectangular patch antenna surrounded by MEBG unit cells to rectangular patch antenna over the proposed MEBG ground are presented in the table VII.

TABLE VII
 COMPARISON OF DESIGNED MODEL RESULTS

Parameter	Conventional Ground	Surrounded MEBG Ground	Underneath MEBG Ground	Proposed MEBG Ground
EBG size	33.3X27.6 mm ²	32.4X27.2m m ²	27.7X22.5 mm ²	27.3X22.1 mm ²
Ground Size	116X59 mm ²	94.3X73 mm ²	93.3X55.5 mm ²	92.3X55.5 mm ²
Patch length miniaturization (%)	Reference	2.7	17	18
Patch width miniaturization (%)	Reference	1.44	18.4	19.9
Resonating Frequency	2.5GHz	2.5GHz	2.5GHz	2.5GHz
Return Loss (dB)	-31.55	-37.72	-36.44	-31.57
Band width (MHz)	63.1	97.7	101.2	130
Fractional band width (%)	2.52	3.9	4.1	5.22

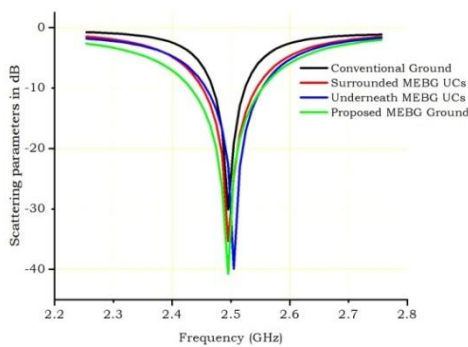
Stacked Electromagnetic Band Gap ground Optimization for low profile patch antenna design

Gain (dB)	1.96	5.59	5.63	6.08
Radiation efficiency (%)	39.6	61.62	60.62	68.25
E plane beam width (Degree)	44.44	52.99	44.87	49.14
H plane beam width (Degree)	37.6	54.7	61.96	57.26
VSWR	1.0543	1.0263	1.0283	1.0525

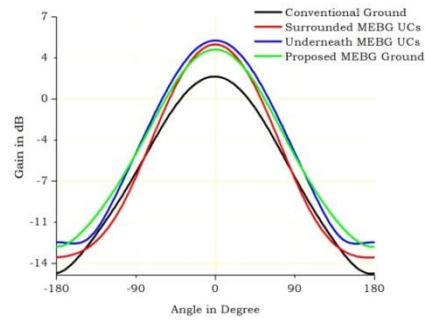
The simulated results of customary MPA (red color), encompassed by MEBG UCs (green color), 3X3 array of MEBG UCs ground lying underneath the patch antenna (blue color) and proposed MEBG ground underneath the patch antenna (yellow color) are appeared in figure 12(a), Figure showing perfect impedance matching between connecting point to the antenna, and all the antennas are resonating at 2.5GHz. The fractional bandwidth of patch antenna over a proposed MEBG ground is more, when contrasted with remaining three strategies (conventional ground, surrounded MEBG UCs, 3X3 array of MEBG ground). Directional E pattern of all the four models are appeared in figure 12(b), conventional MPA (red color) has back radiation of -12dB, front radiation 4.6dB, antenna encompassed by MEBG UCs (blue color) has back radiation of -13dB, front radiation of 5.37dB, ground built by 3X3 array of MEBG UCs lying underneath and covering the entire foot print of the patch antenna (green color) has back radiation of -12dB, front radiation of 5.6dB. Proposed MEBG (figure 11) ground underneath the patch antenna (yellow color) has back radiation of -11.5dB, front radiation of 6.1dB. After comparison, it tends to be inferred that the proposed MEBG structure radiating vast majority of its energy in forward direction, less wastage in reverse heading.

TABLE VIII SUMMARY OF SIMULATED RESULTS OF CONVENTIONAL, SURROUNDED MEBG, 3X3 MEBG ARRAY AND PROPOSED MEBG GROUNDED MODELS.

Ground Structure	Front Radiation	Back Radiation
Conventional Ground	4.6dB	-12dB
Surrounded MEBG	5.37dB	-13dB
3X3MEBG array	5.6dB	-12dB
Proposed MEBG	6.1dB	-11.6dB



(a) Return Loss

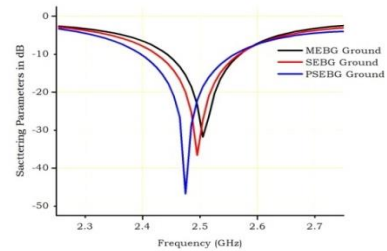


(b) 2D-Gain

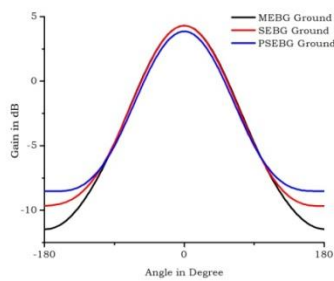
Fig. 12. Simulation results of rectangular patch antenna over the conventional, surrounded MEBG unit cells, 3X3 array of MEBG unit cells and proposed MEBG unit cells grounded models.

In resulting clarifications, the proposed MEBG ground procedure appeared in figure 11 is supplanted first by a ground designed with SEBG UCs and later PSEBG UCs. The new antenna has footprint of 24.3X19.1mm², over the SEBG UCs ground of 92.3X55.5mm² and showing 143.1MHz (fractional band width of 5.73%) bandwidth at 2.5GHz and gain of 6.15dB. In this strategy the measure of radiating patch is additionally scaled down by 27% along its length and 30.7% along its width, band width of 3.21% and gain of 3.22dB improved contrasted with conventional design. Next PSEBG UC ground is embedded instead of proposed MEBG UC ground, the new antenna has footprint of 22.35X17.15mm², over the PSEBG UC ground of 92.3X55.5mm² and showing 167.5MHz (fractional band width of 6.8%) bandwidth at 2.5GHz and gain of 6.13dB. In this technique the size of radiating patch is scaled 32% along its length and 37% along its width. Bandwidth of 3.6% and gain of 1.51dB improved contrasted with traditional design.

The aperture of radiating patch antenna is extremely all around limited in proposed PSEBG ground strategy, but noteworthy larger than the size of PSEBG UC. Further decrease of patch antenna dimensions will make the antenna size littler than the UC size, results PSEBG metallization will get energized by the feed line like antenna. The ground measurements in SEBG and PSEBG models are same as proposed MEBG ground. All models of antennas and its parameters, beginning from MEBG ground to PSEBG ground embedded with patch antenna are portrayed in table VIII, for easy of examination and better to analyze the new SEBG and PSEBG results.



(a) Return Loss



(b) 2D-Gain

Fig. 13. Simulation results of rectangular patch antenna over the proposed MEBG, SEBG and PSEBG grounded models.

TABLE IX SUMMARY OF SIMULATED RESULTS OF THREE EBG MODELS.

Parameter	Surrounded MEBG Ground	Underneath MEBG Ground	Proposed MEBG Ground
EBG size	27.3X22.1 mm ²	24.3X19.1 mm ²	22.35X17.15 mm ²
Ground Size	92.3X55.5 mm ²	92.3X55.5 mm ²	92.3X55.5 mm ²
Patch length miniaturization (%)	18	27	32
Patch length miniaturization (%)	19.9	30.7	37
Resonating Frequency	2.5GHz	2.5GHz	2.5GHz
Return Loss (dB)	-31.57	-36.64	-46.79
Band width (MHz)	130	143.1	167.5
Fractional band width (%)	5.22	5.7	6.8
Gain (dB)	6.08	6.14	6.14
Radiation efficiency (%)	68.25	69.35	70.65
E plane beam width (Degree)	49.14	48.72	47.86
H plane beam width (Degree)	57.26	56.41	53.84
VSWR	1.0525	1.0299	1.009
Front Radiation	6.1dB	6.14dB	6.13dB
Back Radiation	-11.5dB	-9.5dB	-8.5dB

Figure 13(a), demonstrating that all the antennas are entirely coordinated to its power source. All antennas are roughly resonating at 2.5GHz. The factional bandwidth, directivity, radiating efficiency are expanding, the profile of antenna, beam width are diminishing from MEBG ground patch antenna to PSEBG grounded patch antenna. Directional E pattern of three proposed grounded models are appeared in figure 14(b) and its outcomes recorded in table IX. From acquired outcomes it can be concluded that SEBG and PSEBG structures proposed in this paper delivering more enhancement in results than proposed MEBG results, so these two novel structures are well appropriate in design of low profile radiating antenna, additionally accomplish scaling down in ground plane and enhance the forward radiation .

V. CONCLUSION

In this paper the novel (FBG and AMC) properties of EBG are used in improving the radiation attributes of patch antenna and deliver low profile. The MEBG structure is

considered as reference for development of two new stacked structures named as SEBG and PSEBG. The FBG and AMC properties of two new models are derived using FEM based simulator; acquired outcomes are contrasted with reference MEBG model. The principal objective is to choose the best EBG ground for low profile antenna with least back radiation. Amid examination three models of MEBG grounds are considered and its impact on the radiation characteristics of patch antenna is contemplated. Optimization of MEBG UCs ground is replaced by new SEBG and PSEBG UCs grounds. The obtained outcomes demonstrating low profile antenna having more focused radiation pattern in forward direction with minimum back radiation over the proposed new SEBG and PSEBG grounds.

REFERENCES

- Hansen, R. C., *Electrically Small, Super directive, and Superconducting Antennas*, 82-89, New Jersey, 2006.
- Hoorfar, A., "An experimental study of microstrip antennas on very high permittivity ceramic substrates and very small ground planes," *IEEE Trans. Antennas Propagation*, Vol. 49, No. 5, 838-840, May 2001.
- K. Praveen Kumar, Dr. Habibulla Khan "Optimization of EBG structure for mutual coupling reduction in antenna arrays; a comparative study" *International Journal of engineering and technology*, Vol-7, No-3.6, Special issue-06, 2018, page 13- 20.
- K. Praveen Kumar, Dr. Habibulla Khan "Active PSEBG structure design for low profile steerable antenna applications" *Journal of advanced research in dynamical and control systems*, Vol-10, Special issue-03, 2018.
- K. Praveen Kumar, Dr. Habibulla Khan, "Design and characterization of Optimized stacked electromagnetic band gap ground plane for low profile patch antennas" *International journal of pure and applied mathematics*, Vol 118, No. 20, 2018, 4765-4776.
- K. Praveen Kumar, Dr Habibulla Khan " Surface wave suppression band, In phase reflection band and High Impedance region of 3DEBG Characterization" *International journal of applied engineering research (IJAER)*, Vol 10, No 11, 2015.
- Olaode, O. O., "Characterization of meander dipole antennas with a geometry based, frequency-independent lumped element model," *IEEE Antennas and Wireless Propagation Letters*, Vol. 11, 346-349, 2012.
- Ares-Pena, F. J., "Genetic algorithms in the design and optimization of antenna array patterns," *IEEE Trans. Antennas Propagation*, Vol. 47, No. 3, 506-510, March 1999.
- Bilotti, F., A. Toscano, and L. Vegni, "FEM-BEM formulation for the analysis of cavity backed patch antennas on chiral substrates," *IEEE Trans. Antennas Propagat.*, Vol. 51, 306-311, 2003.
- Bilotti, F., A. Toscano, and L. Vegni, "Radiation and scattering features of patch antennas with bianisotropic substrates," *IEEE Trans. Antennas Propagat.*, Vol. 51, 449-456, 2003.
- Scamarcio, G., F. Bilotti, A. Toscano, and L. Vegni, "Broad band U-slot patch antenna loaded by chiral material," *Journal of Electromagnetic Waves and Applications*, Vol. 15, No. 10, 1303-1317, 2001.
- Bilotti, F. and L. Vegni, "Chiral cover effects on microstrip antennas," *IEEE Trans. Antennas Propagat.*, Vol. 51, 2891-2898, 2003.
- Vegni, L., A. Toscano, and F. Bilotti, "Shielding and radiation characteristics of planar layered inhomogeneous composites," *IEEE Trans. Antennas Propagat.*, Vol. 51, 2869-2877, 2003.
- Sievenpiper, D., L. Zhang, R. F. J. Broas, N. Alexopolous, and E. Yablonovitch, "High-impedance electromagnetic surfaces with a forbidden frequency band," *IEEE Trans. Microw. Theory Tech.*, Vol. 47, 2059-2074, 1999.
- Sievenpiper, D., "High-impedance electromagnetic surfaces," Ph.D. Dissertation, UCLA, 1999. Available at www.ee.ucla.edu/labs/photon/thesis/ThesisDan.pdf.

16. Sievenpiper, D., E. Yablonovitch, J. N. Winn, S. Fan, P. R. Villeneuve, and J. D. Joannopoulos, "3D metallo-dielectric photonic crystals with strong capacitive coupling between metallic islands," *Phys. Rev. Lett.*, Vol. 80, 2829-2832, 1998.
17. De Cos, M. E., Y. Alvarez Lopez, and F. Las-Heras Andres, "A novel approach for RCS reduction using a combination of artificial magnetic conductors," *Progress In Electromagnetics Research*, Vol. 107, 147-159, 2010.
18. Chang, C.-S., J.-Y. Li, W.-J. Lin, M.-P. Houg, L.-S. Chen, and D.-B. Lin, "Controlling the frequency of simultaneous switching noise suppression by using embedded dielectric resonators in high-impedance surface structure," *Progress In Electromagnetics Research Letters*, Vol. 11, 149-158, 2009.
19. De Cos, M. E., Y. Alvarez Lopez, R. C. Hadarig, and F. Las-Heras Andres, "Flexible uniplanar artificial magnetic conductor," *Progress In Electromagnetics Research*, Vol. 106, 349-362, 2010.
20. Goussetis, G., A. P. Feresidis, and J. C. Vardaxoglou, "Tailoring the AMC and EBG characteristics of periodic arrays printed on grounded dielectric substrate," *IEEE Transactions on Antennas and Propagation*, Vol. 54, No. 1, 82-89, January 2006.
21. Aminian, A., F. Yang, and Y. Rahmat-Samii, "In-phase reflection and EM wave suppression characteristics of electromagnetic band gap ground planes," *IEEE Antennas and Propagation Society International Symposium*, Ohio, 2003.
22. Hansen, R. C., "Effects of a high-impedance screen on a dipole antenna," *IEEE Antennas and Wireless Propagation Letters*, Vol. 1, 46-49, 2002.
23. Yousefi, L., H. Attia, and O. M. Ramahi, "Broadband experimental characterization of artificial magnetic materials based on a microstrip line method," *Progress In Electromagnetics Research*, Vol. 90, 1-13, 2009.
24. De Cos, M. E., Y. Alvarez, and F. Las-Heras, "Planar artificial magnetic conductor: Design and characterization setup in the RFID SHF band," *Journal of Electromagnetic Waves and Applications*, Vol. 23, No. 11-12, 1467-1478, 2009.
25. Abhari R, Eleftheriades G. V. Metallo-dielectric electromagnetic band gap structures for suppression and isolation of the parallel-plate noise in high-speed circuits. *IEEE Trans. Microw. Theory Tech.*, June 2003, vol. 51, p. 1629 – 1639.
26. Feresidis A. P., Apostolopoulos G, Serfas N, Vardoxoglou J. C. Closely coupled metallodielectric electromagnetic band-gap structures formed by double-layer dipole and tripole arrays. *IEEE Trans. Antennas Propag.*, May 2004, vol. 52, p. 1149 – 1158.
27. F. Yang and Y. Rahmat-Samii, "Applications of Electromagnetic Band-Gap (EBG) Structures in Microwave Antenna Designs," Proc. of 3rd International Conference on Microwave and Millimeter Wave Technology, pp.528–31, 2002.
28. R. Marqués and F. Medina, "An Introductory overview on right-handed metamaterials", Proc. the 27th ESA Antenna Workshop on Innovative Periodic Antennas, Spain, pp. 35-41, 2004.
29. Kovacs P., Raida Z., Lukes Z. "Design and optimization of periodic structures for simultaneous EBG and AMC operation". In *Proceedings of the 16th Conference on Microwave Techniques*. Brno: Czechoslovakia Section IEEE, April 2010, p. 195-198.
30. S. Pal Reddy, "Wide band electromagnetic band gap structures, analysis applications to antennas" PhD Dissertation, 2015.
31. M. Rahman and M. A. Stuchly, "Transmission line – periodic circuit representation of planar microwave photonic bandgap structures," *Microwave Optical Tech. Lett.*, vol. 30, no. 1, pp. 15-19, 2001.
32. Joannopoulos, J. D., S. G. Johnson, J. N. Winn, and R. D. Meade, *Photonic Crystals: Molding the Flow of Light*, 2nd edition, Princeton University Press, 2008.
33. S.G. Mao, C.M. Chen, D.C. Chang, "Modeling of Slow-Wave EBG Structure for Printed-Bowtie Antenna Array," *IEEE antennas and wireless propagation letters*, vol. 1, no. 1, pp. 124-127, 2002.
34. G.K. Palikaras, A.P. Feresidis, J.C. Vardaxogolu, "Cylindrical Electromagnetic Bandgap Structures for Directive Base Station Antennas," *IEEE antennas and wireless propagation letters*, vol. 3, no. 1, pp. 87-89, 2004.
35. Z. Iluz, R. Shavit, R. Bauer, "Microstrip Antenna Phased Array With Electromagnetic Bandgap Substrate," *IEEE Transactions on Antenna and Propagation*, vol. 52, no. 6, pp. pp1446-1453, 2004.
36. H. Nakano, Y. Asano, J. Yamauchi, "A Wire Inverted-F Antenna on a Finite-Sized EBG Material," in *IEEE International Workshop on Antenna Technology: Small Antennas and Novel Metamaterials*, 2005.
37. R. Chantalat, C. Menudier, M. Troubat, E. Arnaud, T. Monediere, M Thevenot, B Jecko, P. Dumon, "Enhanced Two Level EBG Antenna for A High F/D Multibeam Reflector Antenna in Ka Band: Design and Characterization," in *The Second European Conference on Antennas and Propagation*, 2007.
38. S. Zhu, R. Langley, "Dual-Band Wearable Textile Antenna on an EBG Substrate," *IEEE Transactions on Antenna and Propagation*, vol. 57, no. 4, pp. 926-935, 2009.
39. S. Kwak, D.U. Sim, J. H. Kwon, "Design of Optimized Multilayer PIFA With the EBG Structure for SAR Reduction in Mobile Applications," *IEEE transactions on electromagnetic compatibility*, vol. 53, no. 2, pp. 325-331, 2011.
40. Su Y, Xing L, Cheng ZZ et al (2010) Mutual coupling reduction in microstrip antennas by using dual layer uniplanar compact EBG (UC-EBG) structure[J]. *IEEE International conference on microwave and millimeter wave technology*, pp 180–183
41. Jing Liang, Hung Yu David Yang " Radiation characteristics of microstrip patch antenna over an electromagnetic band gap surface" *IEEE transactions on antennas and propagation*, vol. 55, no. 6, 2007.
42. Peter Kovacs, Jan Pukely " Stacked high impedance surface for 5GHz WLAN applications" *Radio engineering*, vol. 22, No. 1, 2013.
43. Mohammad MehadiFakharian " Numerical analysis of mushroom like and uniplanar EBG structures utilizing spin sprayed Ni-Co Ferrite films for planar antennas" *European journal of scientific research*, vol 73, no. 1, pp 41-51, 2012.
44. JingkunZeng " Compact electromagnetic band gap structures and its applications in antenna system" Master's thesis, University of Waterloo, Canada 2013.
45. C.M.Tran, H.Hafdallah Ouslimani, L.Zhou, A.C.Priou " High impedance surfaces based antennas for high data rate communications at 40GHz" *Progress in electromagnetic research C*, vol. 13, 217-229, 2010.
46. Peter Kovacs, Tomas Urbanec " Electromagnetic band gap structures: practical tips and advance for antenna engineers" *Radio engineering*, vol. 21, No.1, 2012.
47. Fangming Cao, Suling Wang "Performance of microstrip patch antenna embedded in electromagnetic band gap structure" *Proceedings of the Chinese intelligent systems conference* volume 2, 2015
48. A. Grbic, G. Eleftheriades, "Periodic analysis of a 2-D negative refractive index transmission line structure," *IEEE Transactions on Antennas and Propagation*, vol. 51, no. 10, pp. 2604-2611, 2003.
49. G. Eleftheriades, K. G. Balmain, *Negative Refraction Metamaterials: Fundamental Principles and Applications*, New York: Wiley-IEEE Press, 2005.

AUTHORS PROFILE



P. Saleem Akram was born in India, A.P. He received M.Tech (Communication Engg) from VIT University, Vellore, India in 2008. His research area is Antennas (Metamaterial for WSN applications). He is pursuing his Doctorate from GITAM University, Visakhapatnam, A.P, INDIA. At present working as Asst. Professor at KLEF, Vaddeswaram, Guntur (D.T) in ECE department. He participated in several workshops and conferences.



Dr. T. V. Ramana was born in India. At present he works as Associate Professor in ECE Dept. at GITAM University, Visakhapatnam, A.P, India. His research area is Satellite Communications. His research articles were published in various National & International Journals.